

TKE maps and power spectrum agree for $f_e = 400$ Hz. In addition, the organized motions appear fairly consistent throughout the mixing layer. However, if one examines the TKE maps for $f_e = 200$ Hz, the f_p of the organized vortical structures is nominally 300 Hz. This may be a result of the smearing that can occur when phase locking is employed.⁵ For the most part f_p estimated from the TKE maps lie within a band of frequencies from 270 to 350 Hz.

References

- ¹Vandsburger, U., and Ding, C., "Self-Excited Wire Method for the Control of Turbulent Mixing Layers," *AIAA Journal*, Vol. 33, No. 6, 1995, pp. 1032–1037.
- ²Fiedler, H. E., and Mensing, P., "The Plane Turbulent Shear Layer with Periodic Excitation," *Journal of Fluid Mechanics*, Vol. 150, 1985, pp. 281–309.
- ³Veynante, D., Candel, S. M., and Martin, J.-P., "Influence of the System Response on the Coherent Structures in a Confined Shear Layer," *Physics of Fluids*, Vol. 29, No. 12, 1986, pp. 3912–3914.
- ⁴Ho, C.-M., and Huerre, P., "Perturbed Free Shear Layers," *Annual Review of Fluid Mechanics*, Vol. 16, 1984, pp. 365–424.
- ⁵Disimile, P. J., "The Effect of Ensemble Averaging on Transverse Vorticity Measurements in Forced Shear Flows," *AIAA Journal*, Vol. 24, No. 10, 1986, pp. 1621–1627.

Reynolds Number Effects on the Prediction of Velocity Profile in Compressible Flows

Fariborz Motallebi*
Delft University of Technology,
2629 HS Delft, The Netherlands

IN a recent article, Huang et al.¹ presented an algorithm for the prediction of skin friction and velocity profiles for compressible turbulent boundary layers. Their method relies on the use of an analytical expression for the mean-velocity profile of compressible turbulent boundary layers, based on the van Driest formulation² and the Coles' law of the wake³:

$$\frac{u^+}{u_\tau} = \int_0^{y^+} \frac{2}{1 + \sqrt{1 + 4k^2(y^+)^2[1 - \exp(-y^+/A^+)]^2}} dy^+ + \frac{\Pi}{k} w \left(\frac{y}{\delta} \right) \quad (1)$$

In the above relation, A^+ is the damping factor, k the slope for the law of the wall, $y^+ = yu_\tau/\nu_w$, Π the wake parameter as suggested by Cebecchi and Smith⁴ [$\Pi = 0.55[1 - \exp(-0.243z_1^{0.5} - 0.298z_1)]$], in which $z_1 = Re_\theta/425 - 1$, $w(y/\delta) = 1 - \cos[\pi(y/\delta)]$ the wake function, $u_\tau = \sqrt{(\tau_w/\rho_w)}$ the friction velocity, and the transformed velocity is defined by

$$u^* = (u_\delta/b) \sin^{-1} \left\{ [2b^2(u/u_\delta) - a] / (a^2 + 4b^2)^{0.5} \right\} \quad (2)$$

in which

$$a = (T_\delta/T_w) [1 + r(\gamma - 1)M_\delta^2/2] - 1 \quad (2a)$$

$$b^2 = r(\gamma - 1)M_\delta^2(T_\delta/T_w)/2 \quad (2b)$$

where T is the temperature, r the temperature recovery factor, γ the specific heat ratio, M the Mach number, and the subscripts w

and δ refer to the conditions at the wall and at the edge of the boundary layer. Then, for a given flow condition with a specific boundary-layer momentum thickness θ (or boundary-layer displacement thickness δ^*) as the only known parameter and by using Eq. (1) and the inverse of the van Driest transformation [Eq. (2)] in an iterative procedure, they demonstrated that a unique solution for the skin friction coefficient and, hence, the velocity profile can be obtained. Although their analysis is based on the validity of the van Driest transformation for general compressible flows and direct extension of the wake-function concept from incompressible turbulent boundary-layer data to compressible flows, it does produce, as was stated by Huang et al.,⁵ satisfactory results when applied to a series of experimental data for different freestream Mach numbers, both in terms of skin friction and velocity profile. The speed at which the solution is converged in mathematical sense was also very satisfactory. However, as it will be shown for a given flow Mach number, this method fails to correctly predict the effect of Reynolds number on the mean flow distribution in the boundary layer, and it appears that the accuracy of the method is Reynolds-number dependent. As examples, the effect of Reynolds number on the accuracy of the results can be observed in Figs. 1–6 for three different flow Mach numbers. Experimental data examined here are taken from Winter and Gaudet⁶ for $M_\delta = 1.4$ and $Re_\theta = 17 \times 10^3 \rightarrow 130 \times 10^3$ (Figs. 1 and 2), $M_\delta = 2.2$ and $Re_\theta = 14 \times 10^3 \rightarrow 90 \times 10^3$ (Figs. 3 and 4), and Stalmach⁷ for $M_\delta = 3.68$ and $Re_\theta = 2 \times 10^3 \rightarrow 10.5 \times 10^3$ (Figs. 5 and 6). As can be seen, there exists strong Reynolds number influence on the prediction of mean-velocity profiles. For all the cases, their method fails to correctly predict the velocity profiles at

Table 1 Percent error (ΔC_f) in the prediction of skin friction coefficient by the method of Huang et al.,¹ $\Delta C_f = (1 - C_{f,calc}/C_{f,exp}) \times 100$

Profile	Ref.	M_δ	Re_θ	Predicted $\Delta C_f, \%$
10	6	1.394	17,914	0.2
11	6	1.395	39,333	1.7
12	6	1.400	60,234	2.0
13	6	1.400	113,948	2.0
14	6	1.400	128,035	2.2
JPL-A112	8	1.314	19,880	2.0
JPL-A113	8	1.321	21,236	2.3
JPL-A114	8	1.320	21,971	2.9
JPL-A115	8	1.315	23,580	2.6
JPL-A122	8	1.308	34,560	2.7
65020301	7	2.865	225,909	2.8
65020401	7	2.897	167,222	2.3
65020501	7	2.908	50,857	2.8
65020601	7	2.910	49,261	3.2
74021801	7	4.517	10,134	-5.4
74021802	7	4.510	15,882	-7.2
74021803	7	4.510	19,789	-5.8
74021804	7	4.500	25,001	-6.1
74021805	7	4.493	28,447	-7.5
58020201	7	2.735	2,011	7.7
58020203	7	2.731	3,834	5.4
58020207	7	2.739	12,228	-5.2
18	6	2.186	14,640	-2.3
19	6	2.197	30,865	-2.3
20	6	2.201	48,223	-2.7
21	6	2.206	88,907	-0.5
39	6	2.198	19,939	-1.9
40	6	2.199	24,993	-2.5
41	6	2.200	30,300	-2.5
42	6	2.201	35,014	-2.2
43	6	2.202	39,867	-2.1
44	6	2.204	46,899	-2.3
45	6	2.205	53,841	-1.5
46	6	2.206	63,569	-1.8
47	6	2.207	73,310	-1.1
48	6	2.208	84,259	-0.4
JPL-A132	8	2.172	23,938	3.5
JPL-A133	8	2.166	24,409	3.3
JPL-A134	8	2.164	25,782	3.2
JPL-A135	8	2.172	25,891	3.0

Received July 6, 1995; revision received Oct. 30, 1995; accepted for publication Nov. 1, 1995. Copyright © 1995 by the American Institute of Aeronautics and Astronautics, Inc. All rights reserved.

*Research Fellow, Faculty of Aerospace Engineering, Kluyverweg 1; formerly Assistant Professor, Tehran University, Tehran, Iran.

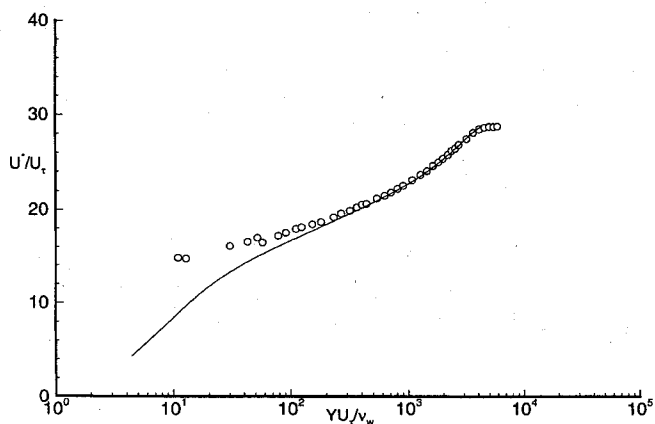


Fig. 1a Transformed velocity profile in semilogarithmic coordinates. Experimental data from Winter and Gaudet,⁶ $M_\delta = 1.3943$, $Re_\theta = 17,914$, profile 10: \circ , experiment and —, Huang et al.

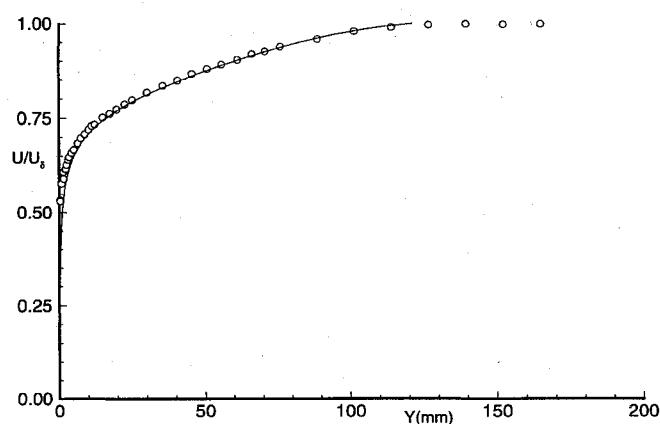


Fig. 1b Untransformed velocity profile in normal coordinates. Experimental data from Winter and Gaudet,⁶ $M_\delta = 1.3943$, $Re_\theta = 17,914$, profile 10: \circ , experiment and —, Huang et al.

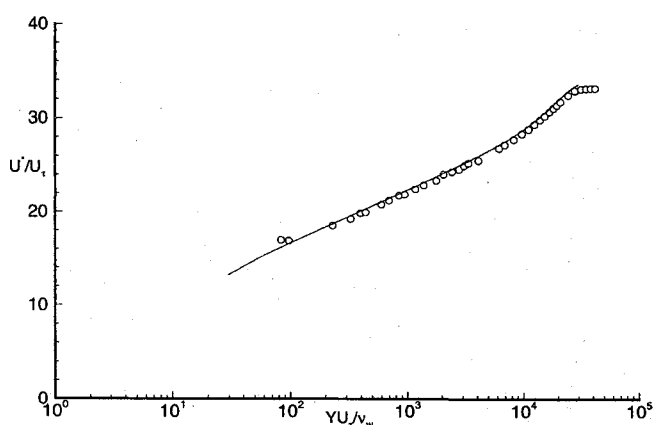


Fig. 2a Transformed velocity profile in semilogarithmic coordinates. Experimental data from Winter and Gaudet,⁶ $M_\delta = 1.4003$, $Re_\theta = 128,035$, profile 14: \circ , experiment and —, Huang et al.

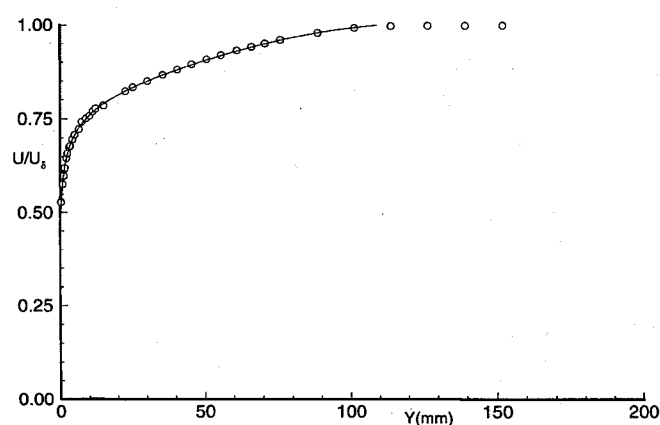


Fig. 2b Untransformed velocity profile in normal coordinates. Experimental data from Winter and Gaudet,⁶ $M_\delta = 1.4003$, $Re_\theta = 128,035$, profile 14: \circ , experiment and —, Huang et al.

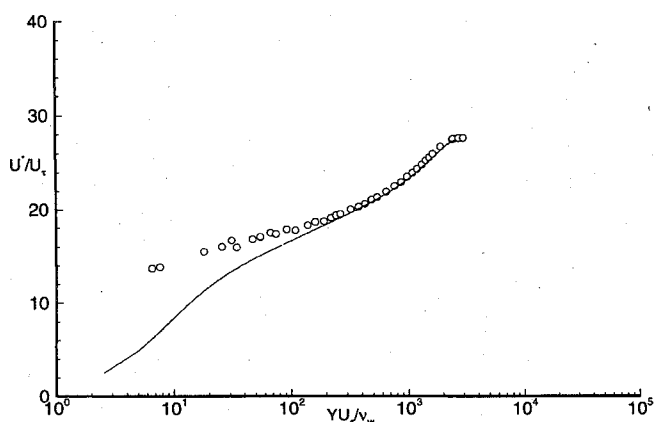


Fig. 3a Transformed velocity profile in semilogarithmic coordinates. Experimental data from Winter and Gaudet,⁶ $M_\delta = 2.1865$, $Re_\theta = 14,640$, profile 18: \circ , experiment and —, Huang et al.

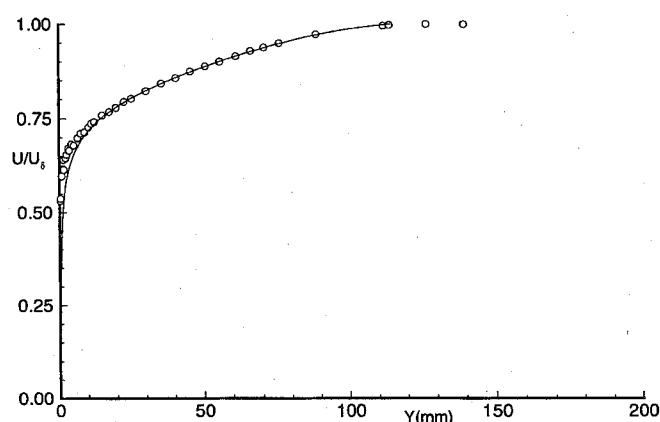


Fig. 3b Untransformed velocity profile in normal coordinates. Experimental data from Winter and Gaudet,⁶ $M_\delta = 2.1865$, $Re_\theta = 14,640$, profile 18: \circ , experiment and —, Huang et al.

the lower range of Reynolds numbers. But as the Reynolds number increases, the difference between the predicted velocity profile and the experimental data decreases. Note that although the wake parameter Π in the Stalmach's experiment⁷ varies from 0.4464 to 0.5499 (low-Reynolds-number effect), this variation does not compensate for the effect of Reynolds number on the whole predicted velocity profile. For the other two sets of data, the wake parameter Π is practically constant and could not influence this behavior (the wake parameter depends strongly on Re_θ only for small Reynolds

numbers). The percent error in the prediction of skin friction coefficient ΔC_f [i.e., $\Delta C_f = (1 - C_{f,calc}/C_{f,exp}) \times 100$ where $C_{f,calc}$ and $C_{f,exp}$ are, respectively, calculated and experimental values of skin friction coefficient] as calculated by their method for a number of experimental data⁶⁻⁸ is given in Table 1. In contrast to the predicted velocity profile, ΔC_f is not very sensitive to the variation of Re_θ . This strong dependence on the Reynolds number, which is only observed in the predicted velocity profile, suggests that at least for supersonic flows (i.e., $M_\delta > 1.0$) the expression used for

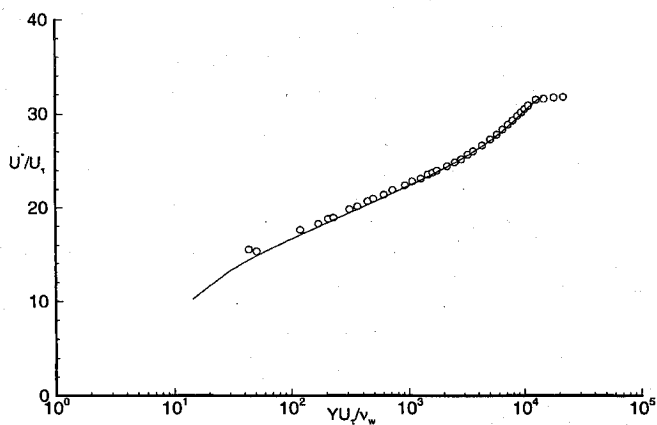


Fig. 4a Transformed velocity profile in semilogarithmic coordinates. Experimental data from Winter and Gaudet,⁶ $M_\delta = 2.2064$, $Re_\theta = 88,907$, profile 21: \circ , experiment and —, Huang et al.

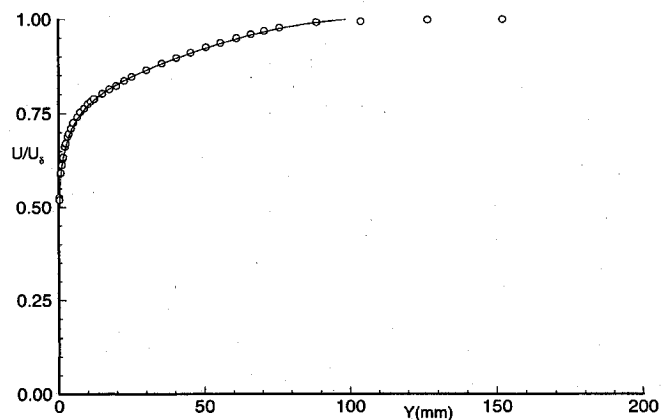


Fig. 4b Untransformed velocity profile in normal coordinates. Experimental data from Winter and Gaudet,⁶ $M_\delta = 2.2064$, $Re_\theta = 88,907$, profile 21: \circ , experiment and —, Huang et al.

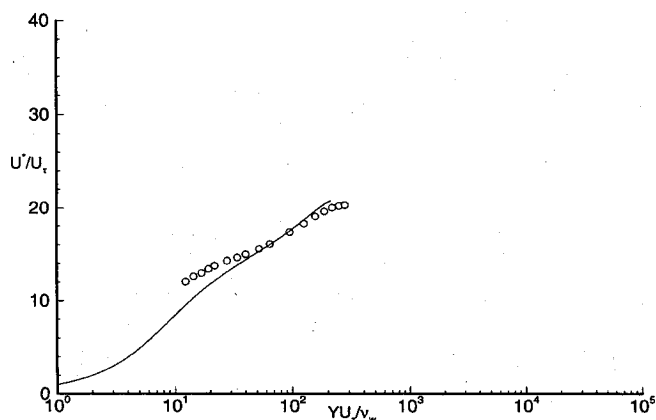


Fig. 5a Transformed velocity profile in semilogarithmic coordinates. Experimental data from Stalmach,⁷ $M_\delta = 3.6840$, $Re_\theta = 2115.3$, case 58020301: \circ , experiment and —, Huang et al.

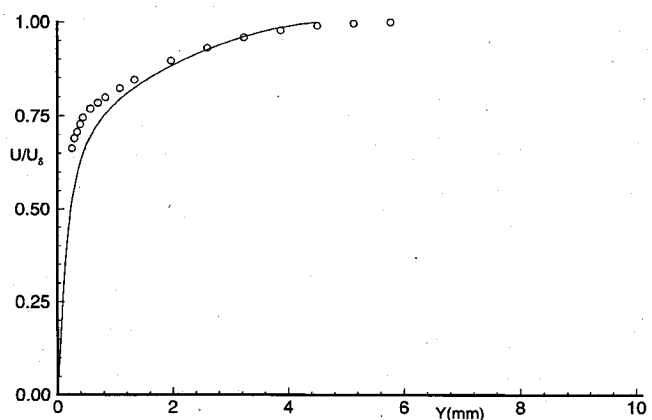


Fig. 5b Untransformed velocity profile in normal coordinates. Experimental data from Stalmach,⁷ $M_\delta = 3.6840$, $Re_\theta = 2115.3$, case 58020301: \circ , experiment and —, Huang et al.

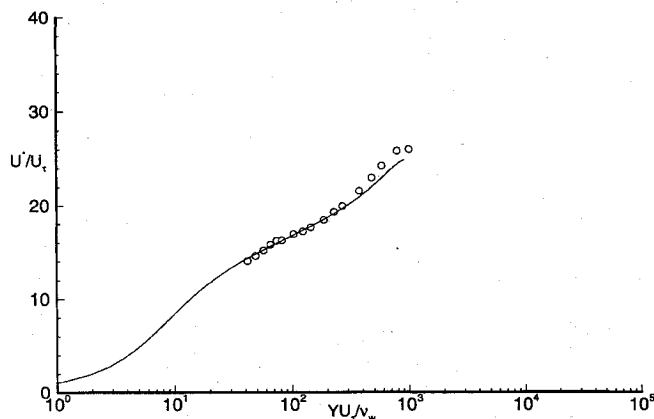


Fig. 6a Transformed velocity profile in semilogarithmic coordinates. Experimental data from Stalmach,⁷ $M_\delta = 3.681$, $Re_\theta = 10,484$, case 58020306: \circ , experiment and —, Huang et al.

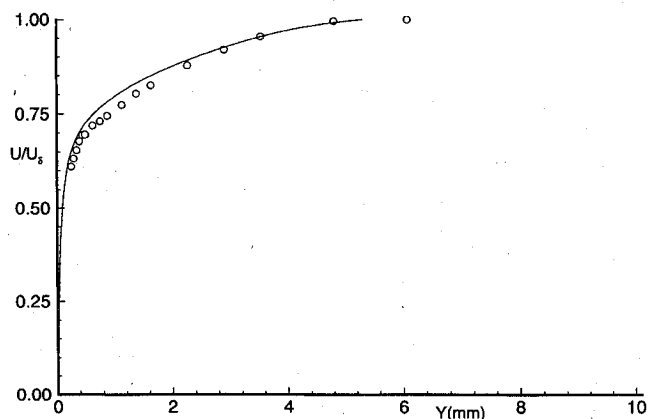


Fig. 6b Untransformed velocity profile in normal coordinates. Experimental data from Stalmach,⁷ $M_\delta = 3.681$, $Re_\theta = 10,484$, case 58020306: \circ , experiment and —, Huang et al.

the transformed mean-velocity profile of turbulent boundary layers [(i.e., Eq. (1))] does not sufficiently represent all of the physical aspects of the mean flow distribution in a compressible turbulent boundary layer. Extra information,^{9,10} or perhaps a more physical approach to the formulation of the mean structure of compressible turbulent boundary layers, is required to achieve complete (physical and mathematical) convergence before it can be applied successfully in any method for the prediction of the mean flow behavior of compressible turbulent boundary layers.

References

- Huang, P. G., Bradshaw, P., and Coakley, T. J., "Skin Friction and Velocity Profile Family for Compressible Turbulent Boundary Layers," *AIAA Journal*, Vol. 31, No. 9, 1993, pp. 1600–1604.
- Van Driest, E. R., "Turbulent Boundary Layer in Compressible Fluids," *Journal of Aeronautical Sciences*, Vol. 18, No. 5, 1951, pp. 145–160.
- Coles, D. E., "The Law of the Wake in the Turbulent Boundary Layers," *Journal of Fluid Mechanics*, Vol. 1, Pt. 2, 1956, pp. 191–226.
- Cebecci, T., and Smith, A. M. O., *Analysis of Turbulent Boundary Layers*, 1st ed., Academic, New York, 1974, pp. 146–148.

⁵Huang, P. G., Bradshaw, P., and Coakley, T. J., "Reply by the Authors to F. Motallebi," *AIAA Journal*, Vol. 32, No. 9, 1994, p. 1939.

⁶Winter, K. G., and Gaudet, L., "Turbulent Boundary Layer Studies at High Reynolds Numbers at Mach Numbers Between 0.2 and 2.8," Aeronautical Research Council, ARC R&M 3712, London, Dec. 1970.

⁷Fernholz, H. H., and Finley, P. J., "A Critical Compilation of Compressible Boundary Layer Data," AGARDograph 223, June 1977.

⁸Collins, D. J., Coles, D. E., and Hicks, J. W., "Measurements in the Turbulent Boundary Layer at Constant Pressure in Subsonic and Supersonic Flow, Part I: Mean Flow," Jet Propulsion Lab., California Inst. of Technology, AEDC-TR-78-21, Pasadena, CA, May 1978.

⁹Motallebi, F., "Comment on 'Skin Friction and Velocity Profile Family for Compressible Turbulent Boundary Layers,'" *AIAA Journal*, Vol. 32, No. 9, 1994, p. 1938.

¹⁰Motallebi, F., "Prediction of Mean Flow Data for Adiabatic 2-D Compressible Turbulent Boundary Layers," Faculty of Aerospace Engineering, Delft Univ. of Technology, Rept. LR-784, Delft, The Netherlands, Feb. 1995.

Reply by the Authors to F. Motallebi

P. G. Huang*

MCAT, Inc., San Jose, California 95127

P. Bradshaw†

Stanford University, Stanford, California 94305

and

T. J. Coakley‡

NASA Ames Research Center,

Moffett Field, California 94035

MOTALLEBI argued that the velocity-profile family of Huang et al.¹ failed to predict the boundary layer at low Reynolds numbers. His argument was based on the observation of experimental data of Winter and Gaudet⁶ and Stalmach.⁷ In particular, in Figs. 3a ($M_\delta = 2.2$, $Re_\theta = 14,640$) and 5a ($M_\delta = 3.7$, $Re_\theta = 2115$), the data close to the wall show higher velocity values than those predicted by the profile family of Huang et al. Motallebi attributed the failure to predict the velocity profile near the wall as "Reynolds number influence" and argued that extra information is needed to explain the low Reynolds number behavior. In his comments, he cited his own reference (Ref. 9) as the source of the explanation for the extra information. But Ref. 9 was simply a letter to the authors to enquire how to get a converged solution with the conditions specified in Huang et al.¹ and the only relevant remark was "More explanations were needed." Now, the velocity profile in a zero-pressure-gradient boundary layer is uniquely defined by any chosen thickness (plus the Reynolds number based thereon) and by the Mach number and heat-transfer parameter. Our velocity-profile family does, of course, need various pieces of empirical information (e.g., the Van Driest transformation and the useful fact that the wake parameter is nearly independent of Mach number). Motallebi apparently failed to observe that although the Reynolds number in Fig. 6a ($M_\delta = 3.7$, $Re_\theta = 10,484$) is smaller than that of Fig. 3a, the data in Fig. 6a show a good match to the predicted profile. Note that although the freestream Mach number in Fig. 6a is larger than that in Fig. 3a, the increase of the freestream Mach number tends to

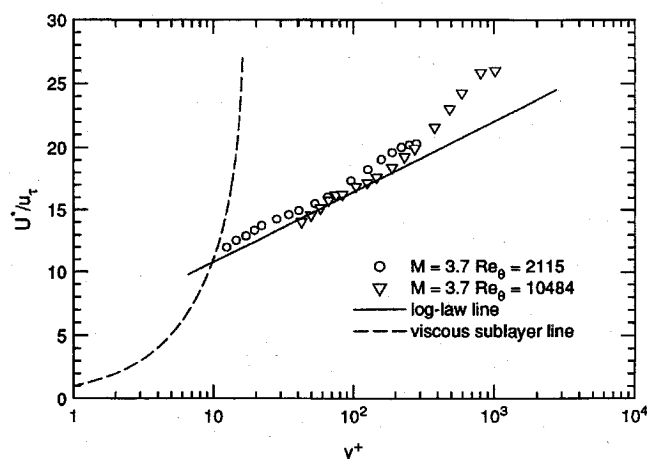


Fig. 1 Transformed velocity profiles (experimental data of Stalmach).

reduce the effective Reynolds number (see Huang et al.¹ for further discussion).

Near the wall (say, $y^+ < 5$), all experimental data have to satisfy

$$\frac{dU^+}{dy^+} = \frac{\mu_w}{\mu} \quad (1)$$

By applying the Van Driest transformation to Eq. (1) and performing the integration from the wall following the assumption that $\mu_w/\mu = (T_w/T)^{0.7}$, one may get a sublayer transformed velocity profile as a function of molecular Prandtl number Pr and two dimensionless parameters

$$M_\tau \left\{ \equiv \frac{u_\tau}{a_w} = \frac{u_\tau}{\sqrt{(\gamma - 1)c_p T_w}} \right\}$$

and

$$B_q \left(\equiv \frac{q_w}{\rho_w c_p u_\tau T_w} \right)$$

(the details of the viscous-sublayer analysis are discussed in Huang and Coleman²). Away from the wall ($y^+ > 30$), experimental evidence indicates that the data are good collapse to the incompressible law of the wall line, when the velocity is transformed to the Van Driest variable.

It is difficult to believe that the experimental data quoted by Motallebi, which show log-law regions for y^+ as low as 7 (see Fig. 3a, the lower limit usually quoted is 30–50), are entirely correct. Here, for purpose of illustration, the data of Stalmach are plotted (cases 58020301 and 58020306) in Fig. 1. In the figure, both log-law and viscous-sublayer lines are also shown. In our opinion, the main cause of the discrepancy between data and our predicted profiles is experimental error or scatter—these are rather old data!—rather than an insufficient number of parameters or missing physical information in our analysis, as suggested by Motallebi.

Motallebi seems to overlook many other low Reynolds number compressible flow data included in Ref. 7, which show well-behaved sublayer and buffer-zone characteristics. Perhaps the most interesting comparison of the low Reynolds number compressible near-wall flow can be seen from the paper by Huang and Coleman,² in which the data were obtained from a direct numerical simulation of compressible channel flow. Unlike the data shown by Motallebi, the direct numerical simulation data of Huang and Coleman² clearly showed three distinct regions—the sub, buffer, and log layers.

References

- Huang, P. G., Bradshaw, P., and Coakley, T. J., "Skin Friction and Velocity Profile Family for Compressible Turbulent Boundary Layers," *AIAA Journal*, Vol. 31, No. 9, 1993, pp. 1600–1604; also Errata, *AIAA Journal*, Vol. 32, No. 11, 1993, p. 2192.
- Huang, P. G., and Coleman, G. N., "Van Driest Transformation and Compressible Wall-Bounded Flows," *AIAA Journal*, Vol. 32, No. 10, 1994, pp. 2110–2113; also Errata, *AIAA Journal*, Vol. 33, No. 9, 1995, p. 1756.

Received July 6, 1995; accepted for publication Nov. 1, 1995. Copyright © 1996 by the American Institute of Aeronautics and Astronautics, Inc. No copyright is asserted in the United States under Title 17, U.S. Code. The U.S. Government has a royalty-free license to exercise all rights under the copyright claimed herein for Governmental purposes. All other rights are reserved by the copyright owner.

*Senior Scientist; M/S 229-1, NASA Ames Research Center, Moffett Field, CA 94035.

†Professor, Department of Mechanical Engineering.

‡Research Scientist.